MRAC Control Based on the LYAPUNOV Function for DC-DC Buck Converter without Mechanical Sensor

AHMED CHOUYA
University of Djilali Bounâama
Department of Genie Electrical
Khemis-Miliana City, 44 225
ALGERIA

Abstract: In this article, we have studied the Model Reference Adaptive Control (MRAC) of the DC-DC Buck converter without mechanical sensor. One of the commands uses the PI controller and the second is based on the LYAPUNOV function. The stability of the command is proven. The proposed observer estimates the current of the inductor as it has a single tuning parameter ϑ. The simulation results, with the SIMULINK/MATLAB software, of control based on the LYAPUNOV function and the proposed observer are very satisfactory.

Key–Words: DC-DC Buck Converter, PI Regulator, LYAPUNOV function, Model Reference Adaptive Control (MRAC), Observer.

Received: March 19, 2024. Revised: March 9, 2025. Accepted: April 14, 2025. Published: June 4, 2025.

1 Introduction

In recent years, a very significan development of renewable energies has occurred. With its inexhaustible potential and without any negative impact on the environment, renewable energy is an appropriate and accessible technology for economic growth and sustainable development. The study of the renewable energy conversion chain: extraction of primary energy, mechanical conversion, electrical conversion, transformation and network integration, is a basic element for improving the quality of *green* energy production.

Electrical energy production from renewable clean sources is becoming a major revolution [1, 2, 3, 4]. high power efficien y and simple structure, their many end-user applications [5] range from fuel and solar cells [6, 7], electric and hybrid vehicles [8, 9], implementation of Battery/SMES hybrid energy storage systems used in electric vehicles [10], DC microgrids and motor drives [11], portable electronic devices [12], to photovoltaic systems [13] and wind turbine generators [14]. As mentioned in Ref. [5], there are two main control application challenges that must be addressed for the converters to match the source and the load; these energy sources are subject to disturbances and vary due to environmental conditions while each of them has different energy generation characteristics that should be properly addressed.

DC-DC converters are a fairly important part of the conversion chain. They are widely used in connections to storage batteries, photovoltaic systems, wind turbines, hybrid systems. These converters are used to adapt the input voltage of a system to the desired output voltage.

The classical non isolated DC-DC converters, which include the Buck, Boost, Buck-Boost, Cuk, SEPIC (Single Ended Primary Inductance Converter) and Zeta (dual-SEPIC) topologies are inadequate for high-power applications, since only one active switch and one diode are responsible for processing the load power.

There are approaches presented by the literature. we fin nonlinear dynamics of Buck converter [15], design of LQR controller for gain based Buck converter [16], adaptive control with MRAC regulator for DC-DC Buck converter [17], adaptive control with MRAC regulator for DC-DC Buck converter [27], adaptive sensorless control for buck converter with constant power load [18], design and evaluation of a quadratic Buck converter [19], an intelligent adaptive control of DC-DC power Buck converters [20], modeling and analysis of fractional order Buck converter using Caputo-Fabrizio derivative [21], a novel continuous control set model predictive control to guarantee stability and robustness for buck power converter in DC microgrids [22], an Adaptive-Predictive control scheme with dynamic hysteresis modulation applied to a DC-DC buck converter [23].

In this article ; we are going to apply the MRAC control without mechanical sensor on a Buck converter. The next section will be the modeling of the Buck followed by the synthesis of two commands firs based in LYAPUNOV function and second with PI regulator. in the fourth section high gain observer is proposed the results and simulations will be in the fift section and the conclusion in the sixth section.

2 DC-DC Buck Converter Model

The electrical circuit of the buck converter is presented in the figure1(cf.[1]).

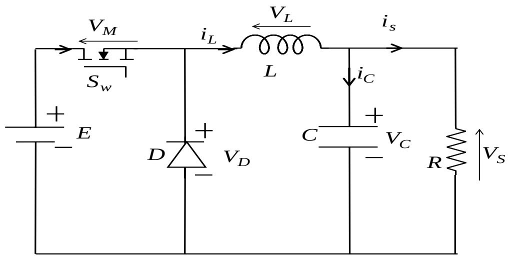

Figure 1: Buck converter diagram.

The equivalent circuit of the buck converter shown in figur 1 is:

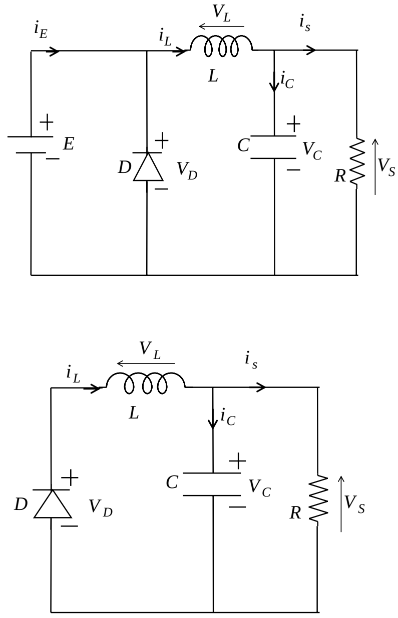

Figure 2: Schematic of the buck converter with S_w closed (over) and S_w opened (under)

During the interval, $t_0 \leq t \leq t_0 + \alpha T$, the switch S_w is closed and the diode D is blocked. The linear model which represents the left configuratio of the circuit describes in figur 2 is given by:

$$\begin{bmatrix} \frac{di_L}{dt} \\ \frac{dV_C}{dt} \end{bmatrix} = \begin{bmatrix} 0 & -\frac{1}{L} \\ \frac{1}{C} & -\frac{1}{RC} \end{bmatrix} \begin{bmatrix} i_L \\ V_C \end{bmatrix} + \begin{bmatrix} \frac{1}{L} \\ 0 \end{bmatrix} E \tag{1}$$

Over the interval, $t_0 + \alpha T \leq t \leq t_0 + T$, S_w is open and the diode D is conducting. The linear model which represents the good configuratio of the circuit described in the figur 2 is given by:

$$\begin{bmatrix} \frac{di_L}{dt} \\ \frac{dV_C}{dt} \end{bmatrix} = \begin{bmatrix} 0 & -\frac{1}{L} \\ \frac{1}{C} & -\frac{1}{RC} \end{bmatrix} \begin{bmatrix} i_L \\ V_C \end{bmatrix} + \begin{bmatrix} 0 \\ 0 \end{bmatrix} E \tag{2}$$

The state space model for the buck converter is shown in equation (3).

$$\begin{bmatrix} \frac{di_L}{dt} \\ \frac{dV_C}{dt} \end{bmatrix} = \begin{bmatrix} 0 & -\frac{1}{L} \\ \frac{1}{C} & -\frac{1}{RC} \end{bmatrix} \begin{bmatrix} i_L \\ V_C \end{bmatrix} + \begin{bmatrix} \frac{E}{L} \\ 0 \end{bmatrix} \alpha \tag{3}$$

3 Design Proposed Controller

3.1 Synthesis of Control with Lyapunov function

In order to ensure zero steady-state error in the output voltage V_C from its reference value V_{ref} , equation (3) is then augmented with another additional state variable x which stands for the integral of the output voltage V_C, the augmented nonlinear state-space model is then given by [24]:

$$\begin{cases} \frac{dx}{dt} = V_C \\ \frac{di_L}{dt} = -\frac{1}{L}V_C + \frac{E}{L}\alpha \\ \frac{dV_C}{dt} = \frac{1}{C}i_L - \frac{1}{RC}V_C \end{cases} \tag{4}$$

The proposed controller design in this work introduces a three states error vector that represents the instantaneous as well as the cumulative errors to assess both transient and robustness criteria. The Overview of proposed control scheme is presented in figur 3.

The error vector comprises the integral of the output voltage tracking error ε_1, the voltage tracking error ε_2, and also the current tracking error ε_3 which are define as

$$\begin{bmatrix} \varepsilon_1 \\ \varepsilon_2 \\ \varepsilon_3 \end{bmatrix} = \begin{bmatrix} \int V_C dt - \int V_{Cref} dt \\ V_C - V_{ref} \\ i_L - i_{Lref} \end{bmatrix} \tag{5}$$

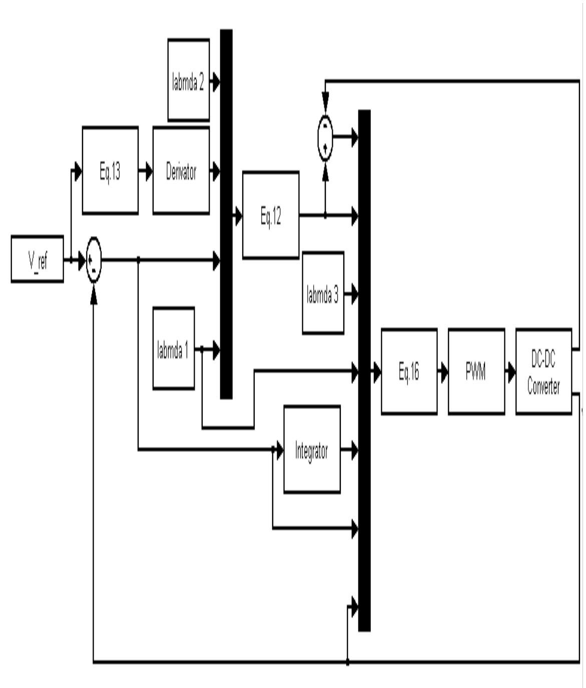

Figure 3: Overview of proposed control scheme.

where i_{Lref} represents the reference current generated by the voltage loop controller, and V_{Cref} represents the desired output voltage of the buck converter.

According to equation (5), the time derivatives of the errors ε_i are derived as

$$\begin{bmatrix} \dot{\varepsilon}_1 \\ \dot{\varepsilon}_2 \\ \dot{\varepsilon}_3 \end{bmatrix} = \begin{bmatrix} \varepsilon_2 \\ \dot{V}_C \\ \dot{i}_L - \dot{i}_{Lref} \end{bmatrix} \tag{6}$$

To prove convergence, let us consider the following LYAPUNOV candidate function:

$$V = \frac{1}{2}\varepsilon_1^2 + \frac{1}{2}(\varepsilon_2 + \lambda_1\varepsilon_1)^2 + \frac{1}{2}\varepsilon_3^2 \text{ with } \lambda_1 > 0 \tag{7}$$

By calculating the derivative time of V, we obtains:

$$\begin{aligned} \dot{V} &= \varepsilon_1\dot{\varepsilon}_1 + (\varepsilon_2 + \lambda_1\varepsilon_1).(\dot{\varepsilon}_2 + \lambda_1\dot{\varepsilon}_1) + \varepsilon_3\dot{\varepsilon}_3 \\ &= \varepsilon_1\varepsilon_2 + (\varepsilon_2 + \lambda_1\varepsilon_1).(\dot{\varepsilon}_2 + \lambda_1\varepsilon_2) + \varepsilon_3\dot{\varepsilon}_3 \\ &= \varepsilon_1(\varepsilon_2 + \lambda_1\varepsilon_1 - \lambda_1\varepsilon_1) \\ &\quad +(\varepsilon_2 + \lambda_1\varepsilon_1).(\dot{\varepsilon}_2 + \lambda_1\varepsilon_2) + \varepsilon_3\dot{\varepsilon}_3 \\ &= -\lambda_1\varepsilon_1^2 + (\varepsilon_2 + \lambda_1\varepsilon_1).(\dot{\varepsilon}_2 + \lambda_1\varepsilon_2 + \varepsilon_1) \\ &\quad +\varepsilon_3\dot{\varepsilon}_3 \\ &= -\lambda_1\varepsilon_1^2 + (\varepsilon_2 + \lambda_1\varepsilon_1). \\ &\quad \left(\frac{1}{C}i_L - \frac{1}{RC}V_C + \lambda_1\varepsilon_2 + \varepsilon_1\right) \\ &\quad +\varepsilon_3\dot{\varepsilon}_3 \end{aligned} \tag{8}$$

According to the third expression of equation (5), we deduce:

$$i_L = \varepsilon_3 + i_{Lref} \tag{9}$$

By replacing expression (9) in equation (8), we have:

$$\begin{aligned} \dot{V} &= -\lambda_1\varepsilon_1^2 + (\varepsilon_2 + \lambda_1\varepsilon_1). \\ &\quad \left(\frac{1}{C}(\varepsilon_3 + i_{Lref}) - \frac{1}{RC}V_C + \lambda_1\varepsilon_2 + \varepsilon_1\right) \\ &\quad +\varepsilon_3\left(\dot{i}_L - \dot{i}_{Lref}\right) \\ &= -\lambda_1\varepsilon_1^2 + (\varepsilon_2 + \lambda_1\varepsilon_1). \\ &\quad \left(\frac{1}{C}i_{Lref} - \frac{1}{RC}V_C + \lambda_1\varepsilon_2 + \varepsilon_1\right) \\ &\quad +\varepsilon_3\left(\frac{1}{C}(\varepsilon_2 + \lambda_1\varepsilon_1) + \dot{i}_L - \dot{i}_{Lref}\right) \end{aligned} \tag{10}$$

If we take

$$\frac{1}{C}i_{Lref} - \frac{1}{RC}V_C + \lambda_1\varepsilon_2 + \varepsilon_1 = -\lambda_2(\varepsilon_2 + \lambda_1\varepsilon_1) \tag{11}$$

Where $\lambda_2 > 0$.
This meant that

$$\begin{aligned} &i_{Lref} = C \\ &\left(-(\lambda_1 + \lambda_2)\varepsilon_2 - (1 + \lambda_1\lambda_2)\varepsilon_1 + \frac{1}{RC}V_C\right) \end{aligned} \tag{12}$$

So

$$\begin{aligned} \dot{V} &= -\lambda_2(\varepsilon_2 + \lambda_1\varepsilon_1)^2 + \varepsilon_3\left(\frac{1}{C}(\varepsilon_2 + \lambda_1\varepsilon_1)\right. \\ &\quad \left. -\frac{1}{L}V_C + \frac{E}{L}\alpha - \dot{i}_{Lref}\right) - \lambda_1\varepsilon_1^2 \end{aligned} \tag{13}$$

By asking

$$\frac{1}{C}(\varepsilon_2 + \lambda_1\varepsilon_1) - \frac{1}{L}V_C + \frac{E}{L}\alpha - \dot{i}_{Lref} = -\lambda_3\varepsilon_3 \tag{14}$$

Where $\lambda_3 > 0$
So

$$\dot{V} = -\lambda_1\varepsilon_1^2 - \lambda_2(\varepsilon_2 + \lambda_1\varepsilon_1)^2 - \lambda_3\varepsilon_3^2 < 0 \tag{15}$$

Thus, the derivative of the LYAPUNOV function (15) is definit negative, which confirm the stability and the convergence of the proposed nonlinear control strategy.

We can deduce the control law

$$\alpha = \frac{L}{E}\left(-\lambda_3\varepsilon_3 - \frac{1}{C}(\varepsilon_2 + \lambda_1\varepsilon_1) + \frac{1}{L}V_C + \dot{i}_{Lref}\right) \tag{16}$$

3.2 Synthesis of Control with PI Regulator

To achieve the purpose of this report, the control strategy is chosen to ensure a constant voltage at the output of the converters. A linear control because of its simplicity is considered. Two cascaded PI correctors are used and then two control loops are created. The external voltage loop compares the voltage reference value and the measured value and imposes a current reference. The internal current loop makes a comparison between the reference and the actual value of the current and the error is corrected to give the duty cycle. A PWM modulator transforms the report into a 0 or 1 pulse command of the converter.

The gains of the PI corrector for voltage are calculated by the pole placement method. Let $G(s)$ be the open loop transfer function. Considering the diagram in figur 4.

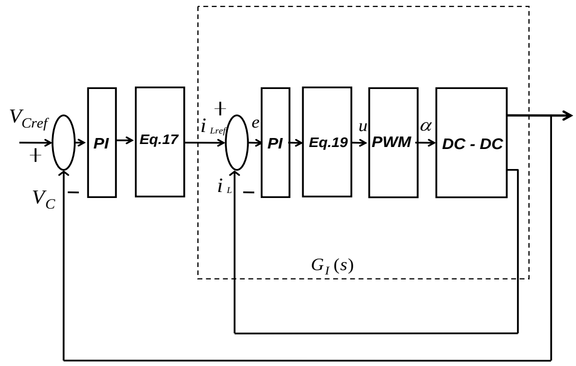

Figure 4: Principle diagram of servoing.

Following the third expression of equation (4); we deduce:

$$i_L = C\left(s + \frac{1}{RC}\right)V_C \tag{17}$$

Or

$$V_C = \frac{\frac{1}{C}}{s + \frac{1}{RC}} i_L \tag{18}$$

One replace V_C in the second formula of equation (4); we have:

$$\alpha = \frac{L}{E} s i_L + \frac{\frac{1}{EC}}{s + \frac{1}{RC}} i_L \tag{19}$$

The figur 4 can be expressed by:

$$G(s) = G_{PI}(s).G_I(s) \tag{20}$$

The transfer functions $G_{PI}(s)$ and $G_I(s)$ are given:

$$G_{PI}(s) = K_P + \frac{1}{sT_i} \tag{21}$$

$$G_I(s) = \frac{1}{1 + sT} \tag{22}$$

Taking $T_i = RC$ and $T \cong 0.8T_i$ the function $G(s)$ is equal to:

$$G_{PI}(s) = \left(K_P + \frac{1}{sT_i}\right)\left(\frac{1}{1 + sT}\right) \tag{23}$$

Then, the closed-loop function $G(s)$ is given:

$$G(s) = \frac{\frac{K_P}{T}\left(s + \frac{1}{T_i K_P}\right)}{s^2 + s\left(\frac{1+K_P}{T}\right) + \frac{1}{TT_i}} \tag{24}$$

The identificatio of the second order characteristic equation; $s^2 + 2\xi\omega s + \omega^2$ is:

$$\omega^2 = \frac{1}{TT_i} \tag{25}$$

$$K_P = 2\xi\omega T - 1 \tag{26}$$

Where the coefficien ω is the bandwidth and ξ is the damping coefficient

4 High Gain Observer for Current Estimation

We intend to construct such an observer, based on the measurement of the out-put voltage [4] the principle is shown in Figure 5.

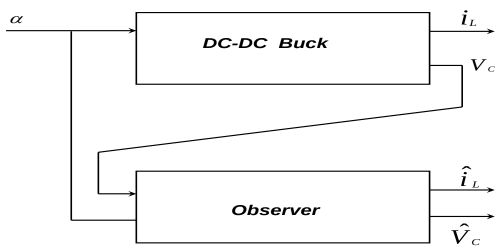

Figure 5: Current observation strategy.

In this part, we are interested in the work presented in [25, 26, 28, 29, 30] which deal with the synthesis of observers with high gain for locally observable systems. Then it is possible to make out the following change of variables:

$$\begin{cases} z_1 = i_L \\ z_2 = -\frac{1}{L}V_C \end{cases} \Leftrightarrow \begin{bmatrix} z_1 \\ z_2 \end{bmatrix} = \begin{bmatrix} 1 & 0 \\ 0 & -\frac{1}{L} \end{bmatrix} \begin{bmatrix} i_L \\ V_C \end{bmatrix} \tag{27}$$

For these changes, model (3) takes the following form:

$$\begin{cases} \frac{dz_1}{dt} = z_2 + \frac{E}{L}\alpha \\ \frac{dz_2}{dt} = \frac{1}{LC}z_1 - \frac{1}{RC}z_2 \end{cases} \tag{28}$$

By imposing

$$z = \begin{bmatrix} z_1 \\ z_2 \end{bmatrix}; \ \mathcal{A} = \begin{bmatrix} 0 & 1 \\ 0 & 0 \end{bmatrix};$$

$$\mathcal{F}(z,\alpha) = \begin{bmatrix} \frac{E}{L}\alpha \\ \frac{1}{LC}z_1 - \frac{1}{RC}z_2 \end{bmatrix}$$

That transforms the nonlinear system (28) into a local system of pyramidal coordinates:

$$\begin{cases} \dot{z} = \mathcal{A}z + \mathcal{F}(z,\alpha) \\ y = Cz \end{cases} \tag{29}$$

With the output vector $C = \begin{bmatrix} 0 & 1 \end{bmatrix}$. Then the following system

$$\dot{\hat{z}} = \mathcal{A}\hat{z} + \mathcal{F}(\hat{z},\alpha) + S_\vartheta^{-1}C^TC(z-\hat{z}) \tag{30}$$

is exponential observer of the system with S_ϑ is the matrix define by:

$$\mathcal{S}_\vartheta = \mathcal{S}_\vartheta^T = \begin{bmatrix} \vartheta^{-1} & -\vartheta^{-2} \\ -\vartheta^{-2} & 2\vartheta^{-3} \end{bmatrix} \tag{31}$$

With $\vartheta > 0$ is the unique solution of the following LYAPUNOV algebraic equation:

$$\vartheta\mathcal{S}_\vartheta + \mathcal{A}^T\mathcal{S}_\vartheta + \mathcal{S}_\vartheta\mathcal{A} = C^TC \tag{32}$$

$S_\theta^{-1}C_1^T$ is the observation gain.

Hypothesis 1. *: The function $\mathcal{F}$ is globally* LIPCHITZIAN *with respect to z uniformly with to α.*

$$\|\mathcal{F}(z,\alpha) - \mathcal{F}(\hat{z},\alpha)\| \le k\,\|z-\hat{z}\| \tag{33}$$

k: LIPSCHITZ *constant*

Hypothesis 2. *:*
Takes us

$$\left|e^T\mathcal{S}_\vartheta\tilde{\mathcal{F}}\right| \le \left\|e^T\right\| \|\mathcal{S}_\vartheta\| \left\|\tilde{\mathcal{F}}\right\| \tag{34}$$

Hypothesis 3. *:*
As

$$\lambda_{\min}(\mathcal{S}_\vartheta)\,\|e\|^2 \le e^T\mathcal{S}_\vartheta e \tag{35}$$

with $\lambda_{\min}(S_\theta)$ is the eigenvalue minimal.

Hypothesis 4. *:*
We consider

$$\vartheta > 2k\frac{\lambda_{\max}(\mathcal{S}_\vartheta)}{\lambda_{\min}(\mathcal{S}_\vartheta)} \ \textit{with} \ k > 0 \tag{36}$$

with $\lambda_{\min}(S_\theta)$; $\lambda_{\max}(S_\theta)$ are the eigenvalues minimal and maximum of S_θ.

4.1 Proof of stability analysis and observer convergence

Consider the error:

$$e = z - \hat{z} \tag{37}$$

Its dynamics is given by:

$$\begin{aligned} \dot{e} &= \mathcal{A}z + \mathcal{F}(z,\alpha) - \mathcal{A}\hat{z} - \mathcal{F}(\hat{z},\alpha) \\ &\quad -S_\vartheta^{-1}C^TC(z-\hat{z}) \\ &= \mathcal{A}(z-\hat{z}) + \mathcal{F}(z,\alpha) - \mathcal{F}(\hat{z},\alpha) \\ &\quad -S_\vartheta^{-1}C^TC(z-\hat{z}) \\ &= \left(\mathcal{A} - S_\vartheta^{-1}C^TC\right)e + \tilde{\mathcal{F}} \end{aligned} \tag{38}$$

Where $\tilde{\mathcal{F}} = \mathcal{F}(z,\alpha) - \mathcal{F}(\hat{z},\alpha)$.

Let's consider the following LYAPUNOV function candidate:

$$V(e) = e^T\mathcal{S}_\vartheta e > 0 \tag{39}$$

Its derivative is

$$\begin{aligned} \dot{V}(e) &= \dot{e}^T\mathcal{S}_\vartheta e + e^T\mathcal{S}_\vartheta\dot{e} \\ &= \left[\left(\mathcal{A} - S_\vartheta^{-1}C^TC\right)e + \tilde{\mathcal{F}}\right]^T\mathcal{S}_\vartheta e \\ &\quad +e^T\mathcal{S}_\vartheta\left[\left(\mathcal{A} - S_\vartheta^{-1}C^TC\right)e + \tilde{\mathcal{F}}\right] \\ &= e^T\mathcal{A}^T\mathcal{S}_\vartheta e - e^TS_\vartheta^{-1}C^TC\mathcal{S}_\vartheta e + \tilde{\mathcal{F}}^T\mathcal{S}_\vartheta e \\ &\quad +e^T\mathcal{S}_\vartheta\mathcal{A}e - e^T\mathcal{S}_\vartheta S_\vartheta^{-1}C^TCe + e^T\mathcal{S}_\vartheta\tilde{\mathcal{F}} \\ &= e^T\left[\mathcal{A}^T\mathcal{S}_\vartheta + \mathcal{S}_\vartheta\mathcal{A}\right]e - 2e^TC^TCe \\ &\quad +2e^T\mathcal{S}_\vartheta\tilde{\mathcal{F}} \\ &= e^T\left[-\vartheta\mathcal{S}_\vartheta + C^TC\right]e - 2e^TC^TCe \\ &\quad +2e^T\mathcal{S}_\vartheta\tilde{\mathcal{F}} \\ &\le -\vartheta e^T\mathcal{S}_\vartheta e + 2e^T\mathcal{S}_\vartheta\tilde{\mathcal{F}} \end{aligned} \tag{40}$$

By taking account of the hypothisis 2 and by introducing the norms, then:

$$\begin{aligned} \dot{V}(e) &\le -\vartheta V(e) + 2\left|e^T\mathcal{S}_\vartheta\tilde{\mathcal{F}}\right| \\ &\le -\vartheta V(e) + 2\left\|e^T\right\| \|\mathcal{S}_\vartheta\| \left\|\tilde{\mathcal{F}}\right\| \end{aligned} \tag{41}$$

Taking the two equations (37) et (33), where the inequality (41) becomes:

$$\begin{aligned}\dot{V}(e) &\leq -\vartheta V(e) + 2k\left\|e\right\|^2 \left\|\mathcal{S}_\vartheta\right\| \\ &\leq -\vartheta V(e) + 2k\frac{V(e)}{\lambda_{\min}(\mathcal{S})}\left\|\mathcal{S}_\vartheta\right\| \\ &\leq -\vartheta V(e) + 2k\frac{V(e)}{\lambda_{\min}(\mathcal{S})}.\lambda_{\max}(\mathcal{S}_\vartheta) \\ &\leq -\left(\vartheta - 2k\frac{\lambda_{\max}(\mathcal{S}_\vartheta)}{\lambda_{\min}(\mathcal{S}_\vartheta)}\right)V(e) \qquad (42)\end{aligned}$$

This guarantees the exponential stability of the observer for $\vartheta > 2k\frac{\lambda_{\max}(\mathcal{S}_\vartheta)}{\lambda_{\min}(\mathcal{S}_\vartheta)}$ this concludes the proof.

4.2 Observer in the initial coordinates

Note that the observation $\hat{i}_L$ and $\hat{V}_C$ of state i_L and V_C of (3), is obtained by:

$$\begin{bmatrix}\hat{i}_L \\ \hat{V}_C\end{bmatrix} = \begin{bmatrix}1 & 0 \\ 0 & -\frac{1}{L}\end{bmatrix}^{-1}\begin{bmatrix}z_1 \\ z_2\end{bmatrix} \qquad (43)$$

The observer expressed an $\hat{i}_L$ and $\hat{V}_C$ is then given by:

$$\begin{bmatrix}\frac{d\hat{i}_L}{dt} \\ \frac{d\hat{V}_C}{dt}\end{bmatrix} = \begin{bmatrix}0 & -\frac{1}{L} \\ \frac{1}{C} & -\frac{1}{RC}\end{bmatrix}\begin{bmatrix}\hat{i}_L \\ \hat{V}_C\end{bmatrix} + \begin{bmatrix}\frac{E}{L} \\ 0\end{bmatrix}\alpha + \begin{bmatrix}1 & 0 \\ 0 & -\frac{1}{L}\end{bmatrix}^{-1}\begin{bmatrix}\vartheta^{-1} & -\vartheta^{-2} \\ -\vartheta^{-2} & 2\vartheta^{-3}\end{bmatrix}^{-1}\begin{bmatrix}0 \\ 1\end{bmatrix}\left(V_C + \hat{V}_C\right) \quad (44)$$

Our observer is:

$$\begin{cases}\frac{d\hat{i}_L}{dt} = -\frac{1}{L}\hat{V}_C + \frac{E}{L}\alpha + 2\vartheta\left(V_C - \hat{V}_C\right) \\ \frac{d\hat{V}_C}{dt} = \frac{1}{C}\hat{i}_L - \frac{1}{RC}\hat{V}_C - \frac{1}{L}\vartheta\left(V_C - \hat{V}_C\right)\end{cases} \qquad (45)$$

This observer is a copy of model, plus a corrective term that is explicitly given. Moreover, its adjustment is done through the choice of a single parameter ϑ.

5 Simulation Results

This work is based on the output voltage and inductor current generated by buck converter. This problem occurs when there are changes in output voltage. This research that will be carried out in a buck converter using a non linear control and PI regulator.
To examine practical usefulness, the proposed regulator has been simulated for a Buck (see [27]), whose parameters are depicted in Table 1.

Parameters	Notation	Value	Unit
Input Voltage	E	26	V
Output Voltage	V_s	13	V
Inductor	L	10	μH
Resistor Load	R	10	Ω
Capacitor	C	10	μF
Normal switching frequency	f	100	KHz
Switch off	Sw	$\alpha = 0$	
Switch off	Sw	$\alpha = 1$	

Table 1: DC-DC buck converter parameters[27].

First, a comparison is made between the two controls, the control based on the LYAPUNOV function and the PI control. ξ must be chosen 0.6 and the output voltage $V_s = 13V$ at time $t = 0.1s$; there is a step of $7V$, it reaches $20V$. Figure 6 shows that the PI control creates overshoots at the instants of voltage changes (see Figure 7). The mean error is equal to $15.2mV$ and the variance 11.69×10^{-2}. On the other hand, the command based on LYAPUNOV function. There are no such overruns. Figure 8 illustrates the error shape of the output voltage with the histogram where the mean error is $6.3mV$ with a variance 8.43×10^{-2} smaller than that of PI control.

Even the inductance current for PI control has overshoots at transition instants but there is no control based on LYAPUNOV function (Figure 9). In Figure 10; the error of the induction current is plotted with its overshoots its average error is $2mA$ and variance 3.3622×10^{-4} shares against the average current error of the LYAPUNOV based control is $1.6mA$ and its variance 5.0725×10^{-5} (Figure 11). Which shows, the control based on the LYAPUNOV function, more efficient

We will observe the inductance current just for the efficien (control based on the LYAPUNOV function). The current observed follows exactly the desired current (Figure 12), the two curves, apart from the transient state, are merged. Where figur 13 shows current error converge to zero . The mean error is $0.7135mA$ and the variance equals 1.0796×10^{-4}

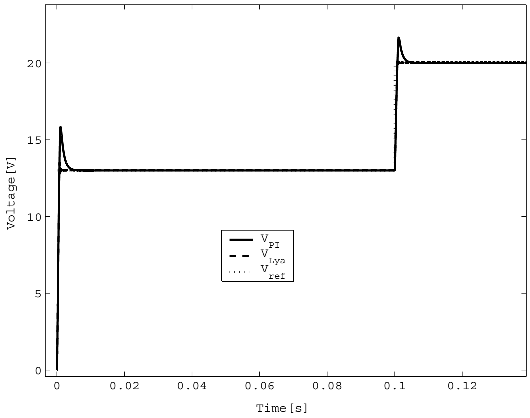

Figure 6: Curves of Voltages.

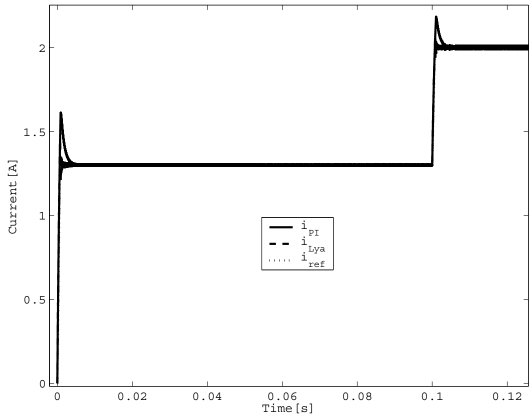

Figure 9: Curves of Currents.

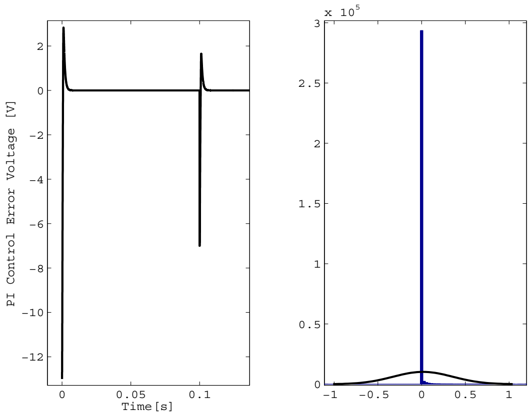

Figure 7: Curves of PI Control Error Voltages with Histogram.

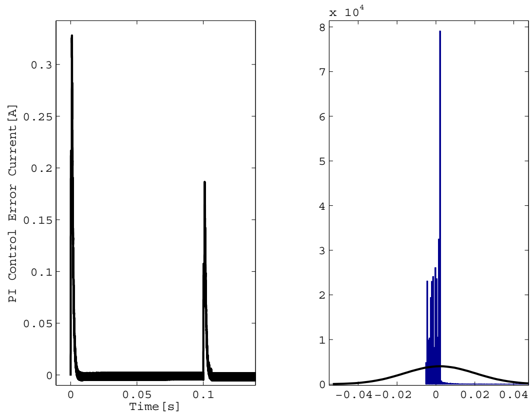

Figure 10: Curves of PI Control Error Currents with Histogram.

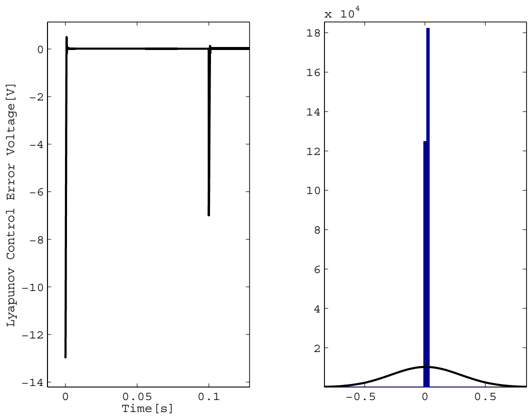

Figure 8: Curves of LYAPUNOV Control Error Voltages with Histogram.

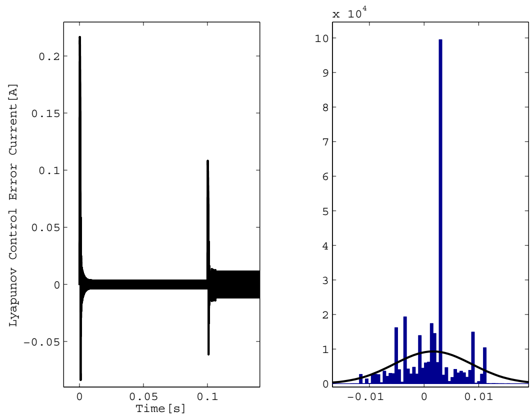

Figure 11: Curves of LYAPUNOV Control Error Currents with Histogram.

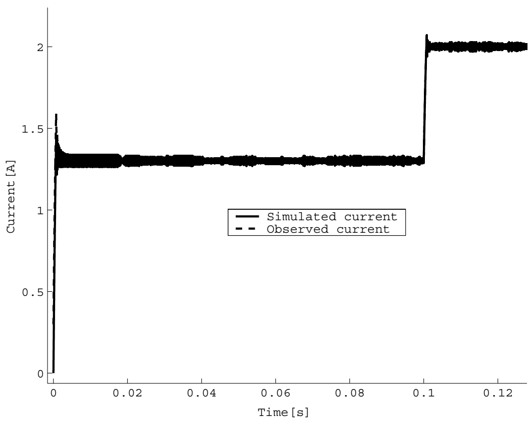

Figure 12: Curves of Simulated and Observed Current.

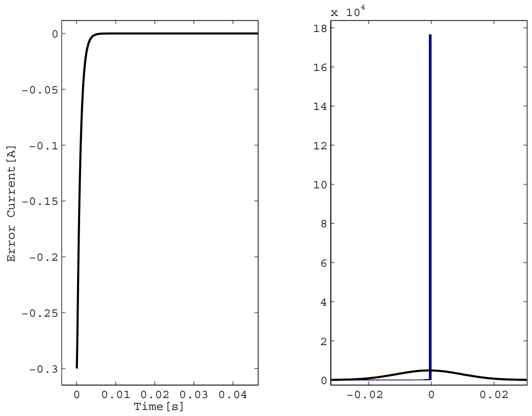

Figure 13: Curves of Error observed Current with Histogram.

6 Conclusion

In this study, the MRAC was used. Where the comparison is made between the PI regulator and the control based on the LYAPUNOV function, the latter performed better than the other. Even, its stability has been proven. The proposed observer has a single ϑ tuning parameter which has the threshold $2k\dfrac{\lambda_{\max}(\mathcal{S}_\vartheta)}{\lambda_{\min}(\mathcal{S}_\vartheta)}$.

References:

[1] A. Dali, S. Diaf and M. Tadjine. Maximum power tracking and current control for solar photovoltaic system Applications, hybrid dynamical system approach. *Journal of Dynamic Systems, Measurement and Control, Transactions of the ASME*. 2019. Volume141. No9. Art. # 91017. DOI : 10.1115/1.4043556

[2] A. Haque. *Maximum power point tracking (MPPT) scheme for solar photovoltaic system*. Energy Technol Pol 2014; Volume1, No1. pp:115-122.

[3] Kada Boureguig, Ahmed Chouya and Abdellah Mansouri. Power improvement of DFIG wind turbine system using fuzzy-feedback linearization control. *Advances in Green Energies and Materials Technology: Selected Articles from the Algerian Symposium on Renewable Energy and Materials (ASREM-2020)*. pp :63-72. Editor Springer Singapore 2021.

[4] Kada Boureguig, Abdellah Mansouri & Ahmed Chouya. Performance enhancements of DFIG wind turbine using fuzzy-feedback linearization controller augmented by high-gain observer. *International Journal of Power Electronics and Drive System (IJPEDS)*, Vol. 11, No. 1, March 2020, pp. 10-23 ISSN: 2088-8694, DOI: 10.11591/ijpeds.v11.i1. pp10-23.

[5] Mirzaei A, Jusoh A, Salam Z. Design and implementation of high efficien y non-isolated bidirectional zero voltage transition pulse width modulated DC-DC converters. *Energy*. 2012. Volume 47. No1. pp:358-369.

[6] H. Wang, A. Gaillard & D. Hissel. A review of DC-DC converter-based electrochemical impedance spectroscopy for fuel cell electric vehicles. *Renew Energy*. 2019. Volume 141. pp:124-138.

[7] F. Dadouche, O. Bethoux & P Kleider. New silicon thin-fil technology associated with original DC-DC converter: an economic alternative way to improve photovoltaic systems efficien cies. *Energy*. 2011. Volume 36, No3. pp:1749-1757.

[8] S. Pirouzi, J. Aghaei, T. Niknam, M. Shafie Khah & J.P. Vahidinasab. Two alternative robust optimization models for fl xible power management of electric vehicles in distribution networks. *Energy*. 2017. Volume 141. pp:635-651.

[9] B. Yang, T. Zhu, X. Zhang, J. Wang, H. Shu, S. Li & T Yu. Design and implementation of Battery/SMES hybrid energy storage systems used in electric vehicles: a nonlinear robust fractional-order control approach. *Energy* 2020. Volume 191. Art. #116510.

[10] Bo Yang, Tianjiao Zhu, Xiaoshun Zhang # YU Tao .Design and implementation of Battery/SMES hybrid energy storage systems used in electric vehicles: A nonlinear robust fractional-order control approach. *Energy*. Volume 191. No. 4. #116510. November 2019. DOI: 10.1016/j.energy.2019.116510.

[11] Z. Wang, S. Li, Q. Li. Discrete-time fast terminal sliding mode control design for DC-DC buck converters with mismatched disturbances. *IEEE Trans Ind Inf* 2019;Volume 16. No.2. pp:1204-12013.

[12] Y.C. Hsu, C.Y. Ting, L.S. Hsu, J.Y. Lin & C.C. Chen. A transient enhancement DC-DC buck converter with dual operating modes control technique. *IEEE Trans Circ Syst II*: Exp Briefs 2018. Volume 66 No.8. pp:1376-1380.

[13] S. Daraban, D. Petreus & Morel. A novel MPPT (maximum power point tracking) algorithm based on a modifie genetic algorithm specialized on tracking the global maximum power point in photovoltaic systems affected by partial shading. *Energy*. Volume 74. pp:374-388. 2014.

[14] R. F. Melicio, V. M. Mendes & J.P.D.S. Catalao. Comparative study of power converter topologies and control strategies for the harmonic performance of variablespeed wind turbine generator systems. *Energy*. 2011. Volume 36. No.1 pp:520-529.

[15] Dmitry Pikulin. nonlinear dynamics of Buck converter. ISSN 1691-5402 ISBN 978-9984-44-071-2 *Environment. Technology. Resources Proceedings of the 8th International Scientific and Practical Conference*. Volume I1

[16] Miklos CSIZMADIA & Miklos KUCZMANN. Design of LQR controller for gain based Buck converter. *An International Journal for Engineering and Information Sciences*. DOI: 10.1556/606.2020.15.2.4 Vol. 15, No. 2, pp. 37-48. 2020. www.akademiai.com

[17] Ahmed Chouya and Kada Boureguig. Adaptive Control with MRAC Regulator for DC-DC Buck Converter, *International Journal of Control Systems and Robotics*, ISSN: 2367-8917, Volume 7, pp: 13-26, Published: April 1, 2022.

[18] Wei He, Yukai Shang, Mohammad Masoud Namazi & Romeo Ortega. Adaptive sensorless control for buck converter with constant power load. *Control Engineering Practice*. Volume 126, September 2022, Art. #105237.

[19] Siripan Trakuldita, Kaweewat Tattiwongb & Chanin Bunlaksananusorna. Design and evaluation of a Quadratic Buck Converter. *8th International Conference on Power and Energy Systems Engineering (CPESE 2021), 10-12 September 2021, Fukuoka, Japan*. Editor ScienceDirect Energy Reports. Volume 8. 2022. pp:536-543.

[20] Hoda Sorouri, Mostafa Sedighizadeh, Arman Oshnoei & Rahmat Khezri. An intelligent adaptive control of DC-DC power buck converters. *International Journal of Electrical Power and Energy Systems*. Volume 141, October 2022, Art. # 108099.

[21] Ruocen Yang, Xiaozhong Liao, Da Lin # Lei Dong. Modeling and analysis of fractional order Buck converter using Caputo-Fabrizio derivative. *7th International Conference on Power and Energy Systems Engineering (CPESE 2020), 26-29 September 2020, Fukuoka, Japa*. Editor Energy Reports Volume 6, Supplement 9, December 2020, pp:440-445

[22] Jiyao Zhoua, Mustafa Alrayah Hassanc, Jiaxuan Zhange, Zehua Zhanga, Shang Wuf, Mingxuan Houg, Yongjian Lia, Erping Lih # Josep M. Guerreroj. A novel continuous control set model predictive control to guarantee stability and robustness for buck power converter in DC microgrids. *International Conference on Energy Engineering and Power Systems (EEPS2021), August 20-22, 2021, Hangzhou, China*. Editor Energy Reports Volume 7, Supplement 7, November 2021, pp:1400-1415.

[23] Nubia Ilia Ponce de Leon Puig, Dimitar Bozalakov, Leonardo Acho, Lieven Vandevelde # José Rodellar. An Adaptive-Predictive control scheme with dynamic Hysteresis Modulation applied to a DC-DC buck converter. ISA Transactions Volume 105, October 2020, pp:240-255.

[24] Samir Abdelmalek, Ali Dali, Azzeddine Bakdi and Maamar Bettayeb. Design and experimental implementation of a new robust observerbased nonlinear controller for DC-DC buck converters, *Energy*. Volume 213. Art. #118816 , 10 September 2020.

[25] J.P .Caron, and J.P .Hautier. Modélisation et commande de la machine asynchrone , Vol. 10. *Paris: Technip*, 1995.

[26] Ahmed Chouya et al. Etude et mise en oeuvre d'un observateur à grand gain de la machine asynchrone *.Journées Nationales sur l'Electrotechnique et l'Automatique 18-19 décembre 2006, ENSET Oran - ALGERIE. JNEA'2006*.

[27] Ahmed Chouya and Kada Bourguigue. Linear Observer Based Linearizing Control of DC-DC Buck Converter, *WSEAS Transactions on Power Systems*, ISSN / E-ISSN: 1790-5060 / 2224-350X, Volume 16, 2021, Art. #5, pp. 52-60 https://wseas.org/wseas/cms.action?id=23286

[28] Ahmed Chouya. Adaptive sliding mode control with chattering elimination for Buck converter driven DC motor,*WSEAS Trans. Syst. Control*, WSEAS Transactions on Systems, ISSN / E-ISSN: 1109-2777

/ 2224-2678, Volume 22, 2023, Art. #3, p.19-28. DOI: 10.37394/23202.2023.22.3. https://wseas.com/journals/systems/2023/a065102-002(2023).pdf

[29] Ahmed Chouya & Kada Boureguig. Adaptive Control with MRAC Regulator for DC-DC Buck Converter, *International Journal of Control Systems and Robotics*, ISSN: 2367-8917, Volume 7, 2022 ,pp.13-26. Editor International Association of Research and Science. https://www.iaras.org/iaras/home/caijps/adaptive-control-with-mrac-regulator-for-dc-dc-buck-converter

[30] Ahmed Chouya. Adaptive Linearizing Control with MRAC Regulator for DC-DC Boost Converter. *International Journal on Applied Physics and Engineering*. ISSN / E-ISSN: / 2945-0489, Volume 1, 2022, Art. #4. pp : 25-30. DOI: 10.37394/232030.2022.1.4 . https://wseas.com/journals/articles.php?id=7487